ChemComm

FEATURE ARTICLE

View Article Online
View Journal | View Issue

Cite this: *Chem. Commun.*, 2024, **60**, 8008

Mechanistic insights into facilitating reductive elimination from Ni(II) species

Bolin Qiao,[a] Fa-You Lin,[a] Dongmin Fu,[a] Shi-Jun Li,[a] Tao Zhang*[ab] and Yu Lan*[acd]

Received 1st June 2024,
Accepted 5th July 2024

DOI: 10.1039/d4cc02667e

rsc.li/chemcomm

Reductive elimination is a key step in Ni-catalysed cross-couplings, which is often considered to result in new covalent bonds. Due to the weak oxidizing ability of Ni(II) species, reductive eliminations from Ni(II) centers are challenging. A thorough mechanistic understanding of this process could inspire the rational design of Ni-catalysed coupling reactions. In this article, we give an overview of recent advances in the mechanistic study of reductive elimination from Ni(II) species achieved by our group. Three possible models for reductive elimination from Ni(II) species were investigated and discussed, including direct reductive elimination, electron density-controlled reductive elimination, and oxidation-induced reductive elimination. Notably, the direct reductive elimination from Ni(II) species often requires a high activation energy in some cases. In contrast, the electron density-controlled and oxidation-induced reductive elimination pathways can significantly enhance the driving force for reductive elimination, accelerating the formation of new covalent bonds. The intricate reaction mechanisms for each of these pathways are thoroughly discussed and systematically summarized in this paper. These computational studies showcase the characteristics of three models for reductive elimination from Ni(II) species, and we hope that it will spur the development of mechanistic studies of cross-coupling reactions.

1. Introduction

Transition metal-catalysed cross-coupling reactions represent a cornerstone of modern synthetic chemistry, offering an unparalleled toolkit for the assembly of small molecules.[1–5] These methodologies are not only profoundly practical but also extremely versatile, and have been integral to the development of pharmaceuticals, agrochemicals, and organic materials.[6–12] Notably, Pd-catalysed processes initially led the charge in this field.[13] The development of Pd-catalysed cross-coupling

[a] College of Chemistry, and Pingyuan Laboratory, Zhengzhou University, Zhengzhou, Henan, 450001, P. R. China
[b] Institute of Intelligent Innovation, Henan Academy of Sciences, Zhengzhou, Henan, 451162, P. R. China. E-mail: zhangtao@hnas.ac.cn
[c] School of Chemistry and Chemical Engineering, Chongqing Key Laboratory of Chemical Theory and Mechanism, Chongqing University, Chongqing, 401331, P. R. China. E-mail: lanyu@cqu.edu.cn
[d] Pingyuan Laboratory, Xinxiang, Henan, 453007, China

Bolin Qiao

Bolin Qiao is a PhD student under the supervision of Prof. Yu Lan in Zhengzhou University. She obtained her Master's degree in chemistry from Zhengzhou University (2022). Her current research interests are focused on the mechanistic study of transition metal catalysed cross coupling reactions.

Fa-You Lin

Fa-You Lin obtained his Bachelor's degree from Zhengzhou University and is currently pursuing his Master's degree under the guidance of Prof. Yu Lan. His research interests are centered on the mechanistic studies of transition metal catalysed cross coupling reactions.

reactions, such as Suzuki–Miyaura, Heck, and Negishi couplings, has provided chemists with powerful tools to construct complex molecules efficiently.[14–21] These Pd-catalysed reactions are celebrated for their broad substrate scope, and excellent regio- and stereoselectivity, setting a high standard in the arsenal of synthetic chemistry.[22–24]

Ni, with its similar electronic and catalytic properties to Pd, has emerged as a particularly promising candidate in this context.[25–27] The development of Ni-catalysed cross-coupling reactions has been recognized as a pivotal advancement.[28,29] Interestingly, initial insights into Ni-catalysed cross-coupling were fundamentally derived from research into the mechanisms of Pd catalysis.[30–33] In addition to being a more affordable and earth-abundant alternative to Pd catalysts, Ni also exhibits several unique properties that result in differentiated reactivity compared with Pd.[33–35] For example, Ni complexes can adopt both high and low-spin configurations in a variety of oxidation states ranging from Ni(0) to Ni(IV).[36–38] As a relatively unstable intermediate, Ni(I) has a propensity to easily afford radicals. This characteristic renders Ni-catalysed reactions particularly advantageous for performing distinct radical-mediated coupling processes, such as radical halogenation and alkylation, expanding the scope of possible synthetic transformations.[32,39,40] Belonging to the same group as Pd, Ni possesses a lower electronegativity and more potent reductive properties, thereby empowering Ni catalysis systems to effectively activate more inert bonds, such as C–O and C–F bonds.[41,42] This versatility also opens up new pathways for forming $C(sp^3)$–$C(sp^3)$ and C-heteroatom bonds that are challenging or inefficient with Pd catalysts.[31,43–45] These properties have been leveraged in the development of myriad Ni-catalysed transformations to access products with diverse properties and functions.[46]

Reductive elimination, which is a fundamental step in Ni-catalysed cross-coupling reactions, is responsible for the construction of a new covalent bond in the organic product of these processes.[47,48] In many Ni-catalysed cross-couplings, the coupling partner compatibility is dictated by the rate and scope of the reductive elimination step.[49] Reductive elimination from Ni(III) or Ni(IV) species is typically facile.[37,50–52] Conversely, the relatively weak oxidizing ability of Ni(II) species coupled with the higher energy of its 3d orbitals lead a great challenge in the generation of Ni(0) species to achieve the full

Dongmin Fu

Dong-Min Fu obtained his Bachelor's degree from Chongqing University and is currently pursuing his PhD degree under the guidance of Prof. Yu Lan. His research interests are centered on the mechanistic studies of transition metal catalysed reactions and photochemical reactions.

Shi-Jun Li

Shi-Jun Li received his PhD in 2018 under the supervision of Prof. De-Cai Fang at Beijing Normal University. Currently, he is an associate professor in Zhengzhou University. His current research interests are focused on the mechanistic study of transition-metal catalysed cycloaddition reactions.

Tao Zhang

Tao Zhang completed his PhD in 2019 under the supervision of Prof. Yu Lan at Chongqing University. After that, he worked as a postdoctoral researcher in Zhengzhou University (2019–2022). At that time, he moved to the National University of Singapore working with Prof. Yu Zhao as a visiting fellow. He is currently an assistant researcher at the Institute of Intelligent Innovation in Henan Academy of Sciences. His research interests focus on the mechanism study of organic reactions with DFT calculations, Machine learning and artificial intelligence chemistry.

Yu Lan

Yu Lan, PhD, is a distinguished professor of Henan Province, professor of organic chemistry in Zhengzhou University. His research focuses on studying the mechanisms of transition metal catalysis and organic catalysis with theoretical computation to achieve mechanism-guided precision synthesis. Currently, he has co-authored more than 300 papers in the fields of organic chemistry.

catalytic cycle. Moreover, Ni(II) species often manifest in stable tetrahedral or square planar geometries depending on its spin state, which can be further hindered by the steric bulk imposed by ligands.[53] Collectively, these factors result in a high energy barrier of reductive elimination during the Ni(II)/Ni(0) catalytic cycle. On the other hand, low-valent Ni catalysts have exhibited remarkable compatibility with a diverse array of functional groups, facilitating the construction of complex molecular frameworks with high regioselectivity and stereoselectivity.[42,54,55] Generally, cross-coupling with C(sp^2) electrophiles is typically accessible with appropriate ancillary ligands to accelerate the reductive elimination from Ni(II) species.[56,57] Although catalytic C(sp^3)–C(sp^3) cross-coupling *via* a Ni(0)/Ni(II) redox couple remains challenging, it has attracted considerable interest over the past several years.[58,59] A common challenge faced by these low-valent Ni catalytic systems is how to effectively enhance the reactivity of Ni(II) species, reduce the energy barrier of reductive elimination, and facilitate the formation of new covalent bonds (Scheme 1).

From a mechanistic perspective, the distinctive characteristics of Ni catalysts afford a diverse range of mechanistic pathways in Ni-catalysed cross-coupling reactions, including both single-electron and double-electron competing mechanisms. This diversity significantly complicates the modes of reductive elimination from Ni(II) species. As shown in Scheme 2, the direct reductive elimination (mode A) from Ni(II) species involves a concerted three-membered-ring transition state formed between the substrate and Ni, leading directly to the desired product.[60,61] This is the most common reductive elimination pathway in Ni-catalysed cross-couplings. However, this mode of reductive elimination may encounter significant challenges due to the high barrier of this process in some cases. Recently, our group conducted an in-depth mechanistic investigation into the Ni(0)-catalysed C(sp^3)–C(sp^3) cross-coupling.[62] We found that direct reductive elimination occurs from Ni(II) species with a high activation free energy, which significantly impedes the subsequent transformations.

Typically, the reductive elimination process is characterized by electron flow from the substrate to the metal center. During the reaction process, appropriately reducing the electron density of the Ni(II) species can enhance the driving force for reductive elimination, thereby facilitating this process. As shown in Scheme 2, the electron density-controlled reductive elimination

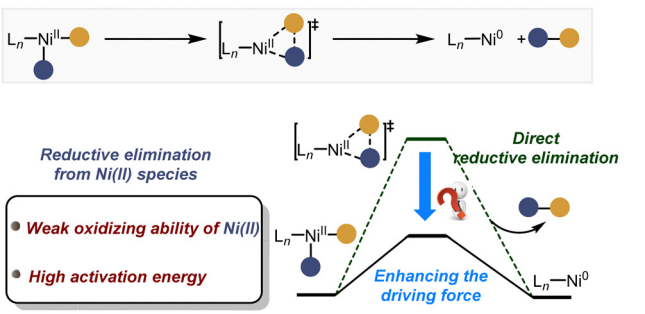

Scheme 1 Challenges for reductive elimination from Ni(II) species.

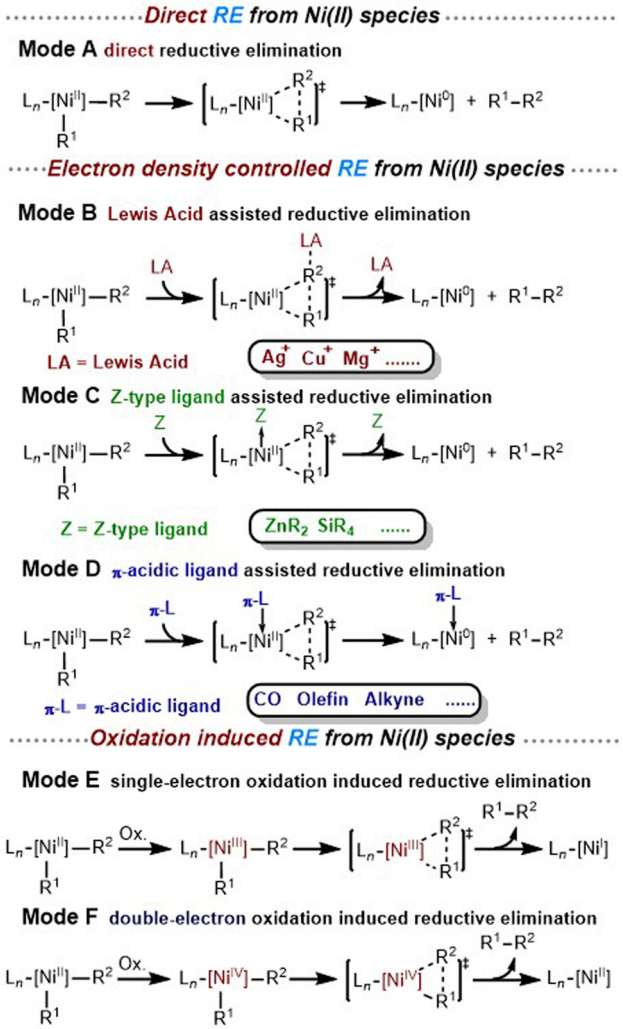

Scheme 2 Possible modes for reductive elimination from Ni(II) species.

provides additional efficacious pathways for the transformation of Ni(II) species. A prevalent approach is Lewis acid-assisted reductive elimination (mode B), where a Lewis acid is introduced into the catalytic cycle to pre-activate the substrate, concurrently modifying the electronic structure and geometric configuration of Ni(II) species, thereby accelerating the reductive elimination process.[56,57,63] Alternatively, Z-type ligand-assisted reductive elimination (mode C) is also determined to be a potential mechanism during this transformation.[62,64,65] In this case, the Z-type metalloligand acts as a σ-acceptor ligand during dative bonding with Ni. A filled d-orbital of Ni provides an electron pair to an unfilled s-orbital of the metalloligand. Z-type coordination reduces the overall electron density of the Ni atom, which could be highly beneficial in facilitating the reductive elimination of Ni(II) species. Moreover, in π-acidic ligand-assisted reductive elimination (mode D), the π-acidic ligands feature either empty or partially filled π* (antibonding) orbitals that can accept electrons from the filled d orbitals of Ni.[58,66–68] Such ligands also play a crucial role in stabilizing the low valent Ni(0) species, resulting in facile reductive elimination during this process.

Beyond the strategy of electron density-controlled reductive elimination, Ni(II) species can be oxidized to Ni(III) or Ni(IV) species, which exhibit strong oxidizing ability. The generation of high-valent metal species most often occurs *via* the processes of oxidative addition, transmetalation.[69–71] However, in nickel-catalysed reactions, these sequences are alterable.[32] This transformation paves the way for a more favorable reductive elimination process, which can be classified as oxidation induced reductive elimination. In this mode, the Ni(II) species can be transformed into Ni(III) species *via* single-electron oxidation, subsequently undergoing reductive elimination to form a new covalent bond with the generation of Ni(I) species (mode E).[72–74] Alternatively, the Ni(II) species may undergo double-electron oxidation to form Ni(IV) species, followed by reductive elimination with the generation of Ni(II) species (mode F).[50,75,76]

Whilst these pathways introduce additional complexity into mechanistic studies, acquiring a deep understanding of the crucial reductive elimination pathways that Ni(II) species might undergo in diverse catalytic systems is critically important. Such insights are essential for the innovative design and development of new type Ni-catalysed cross coupling reactions. Over the past two decades, while numerous reviews have been published concerning experimental studies on Ni-catalysed cross coupling reactions, a profound mechanistic understanding remains elusive.[44,77] Although extensive research has been reported on the reaction mechanisms of such processes, a systematic comprehension is still lacking, particularly with insufficient focus on the key step of reductive elimination.[78,79] In this review, we set aside the experimental aspects and leverage our group's extensive expertise in the mechanistic study of Ni-catalysed coupling reactions to thoroughly elucidate the mechanisms of reductive elimination from Ni(II) species. We mainly focus on two issues: (1) what's the mode of reductive elimination from Ni(II) species and (2) how to promote the reductive elimination from Ni(II) species in catalytic cycles. We anticipate that this review will provide a comprehensive mechanistic perspective for experimental research.

2. The direct reductive elimination from Ni(II) species

The direct reductive elimination mechanism from Ni(II) species is frequently referenced in the context of Ni-catalysed cross-coupling reactions. However, from the mechanistic aspect, Ni(II) species exhibit relatively weak oxidizing ability, resulting in an insufficient driving force for direct reductive elimination. This case is predominantly observed in the formation of $C(sp^2)$–$C(sp^2)$ bonds using Ni-catalysts (Scheme 3).

For example, a combined experimental and theoretical study by Yin and our group reported Ni-catalysed migratory Suzuki–Miyaura cross-coupling.[80] Density functional theory (DFT) calculations shed light on the reaction mechanism (Fig. 1). The direct reductive elimination of Ni(II) species **1** can occur *via* a three-membered ring transition state **2-ts** with an energy barrier of only 14.2 kcal mol^{-1}. The geometry analysis of

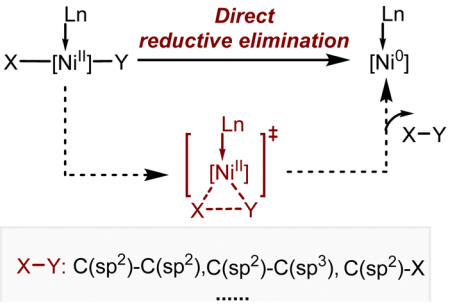

Scheme 3 General mechanism of direct reductive elimination from Ni(II) species.

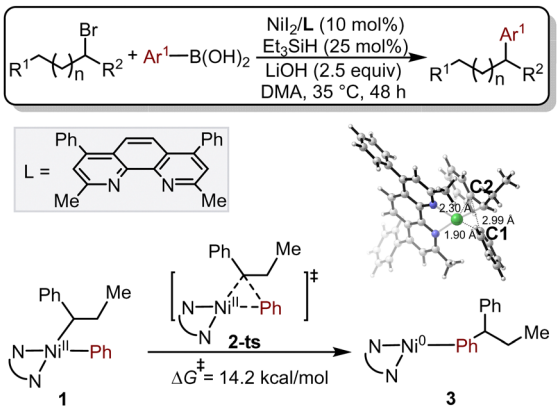

Fig. 1 The model of Ni-catalysed migratory Suzuki–Miyaura cross-coupling and the calculated free energy barrier of reductive elimination. The energies were calculated at the M06/6-311+G(d,p) (LANL2DZ for Ni)/SMD(DMA)//B3LYP/6-31G(d) (LANL2DZ for Ni) level of theory.

transition state **2-ts** is shown in Fig. 1. The bond lengths of C1–Ni, C2–Ni, and C1–C2 bonds are 1.90, 2.30, and 2.99 Å, respectively. The calculated results suggest that direct reductive elimination from Ni(II) species can feasibly proceed for the construction of a new $C(sp^2)$–$C(sp^3)$ bond.

In another case, the Itami and Musaev group performed a theoretical study on the mechanism of Ni-catalysed $C(sp^2)$–$C(sp^2)$ coupling of azoles and naphthalen-2-yl pivalates.[81] As shown in Fig. 2, in the presence of benzoxazole, the Ni(II) species **4** undergoes a concerted metalation deprotonation *via* transition state **5-ts** to afford a Ni(II)-aryl intermediate **6** with concomitant release of PivOH. The direct reductive elimination occurs *via* a three-membered ring-type transition state **7-ts** with an overall energy barrier of 18.0 kcal mol^{-1} (**4** to **7-ts**). In this step, the new $C(sp^2)$–$C(sp^2)$ bond is formed to give the desired product **8**. The computational results further validate the feasibility of direct reductive elimination from Ni(II) species in $C(sp^2)$–$C(sp^2)$ cross-coupling reactions.

Although the mechanism of direct reductive elimination from Ni(II) species can explain the formation of certain chemical bonds in Ni-catalysed cross coupling reactions, it is not universally applicable. For example, the Engle group reported a combined experimental and theoretical study of

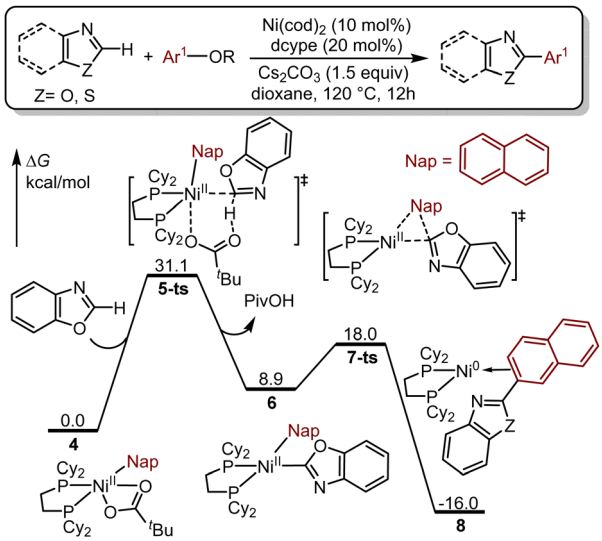

Fig. 2 Free energy profiles of Ni-catalysed 1,2-arylalkylation of olefins with organozinc reagents for direct reductive elimination from Ni(II) species. The energies were calculated at the M06/6-31G(d) (LANL2DZ for Ni)/IEF-PCM(dioxane) level of theory.

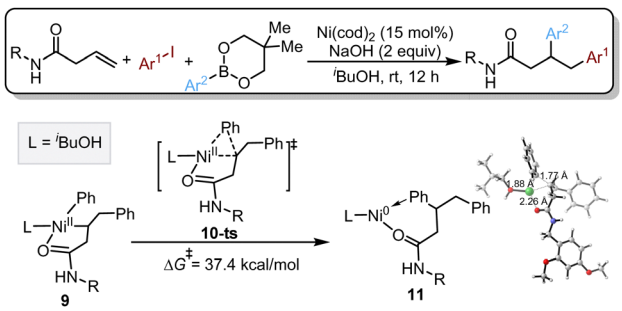

Fig. 3 The model of Ni-catalysed 1,2-diarylation of simple alkenyl amides and the calculated free energy barrier of reductive elimination. The energies were calculated at the M06/6-311+G(d,p) (SDD for Ni)/SMD(tBuOH)//B3LYP/LANL2DZ level of theory.

Ni-catalysed 1,2-diarylation of simple alkenyl amides (Fig. 3).[82] In this reaction, two types of C(sp^2)–C(sp^3) bond are constructed with high region-selectively. However, DFT calculation reveals that the free energy barrier for direct reductive elimination of Ni(II) species **9** is 37.4 kcal mol^{-1}, indicating that the formation of a C(sp^2)–C(sp^3) bond is particularly challenging under this reductive elimination pathway.

3. Electron density controlled reductive elimination from Ni(II) species

The direct reductive elimination of Ni(II) species in Ni-catalysed cross coupling faces multiple challenges, including the stability of its electronic structure, ligand steric effects, energy barriers, the inherent stability of Ni(II) species and its weak oxidizing ability. These factors collectively render the reductive elimination process particularly challenging. Electron density-controlled

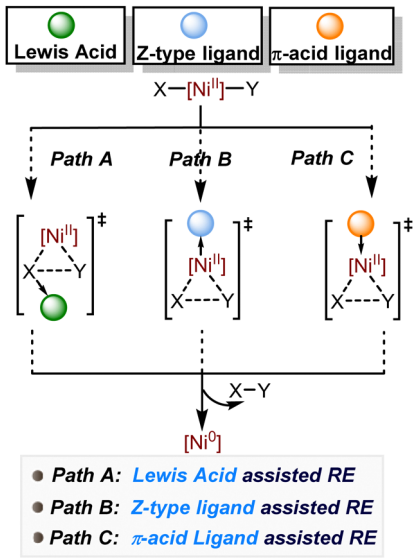

Scheme 4 General mechanism of electron density controlled reductive elimination from Ni(II) species.

reductive elimination can be realized through a multitude of sophisticated strategies aimed at finely tuning the electronic environment of the Ni center (Scheme 4). These methodologies encompass the incorporation of Lewis acids (path A), Z-type ligands (path B), and π-acidic ligands (path C). By enhancing the driving force for the reductive elimination of Ni(II) species, these approaches significantly improve the overall efficiency and selectivity of Ni-catalysed cross-coupling reactions.

3.1. Lewis acid-assisted reductive elimination from Ni(II) species

As a multifaceted modulator in coupling reactions, Lewis acids play a crucial role in reductive elimination of Ni(II) species. By coordinating with reaction intermediates or transition states, Lewis acids can alter the geometry of the Ni center, thereby reducing steric hindrance between ligands. Moreover, it can also lower the electron density of the reacting Ni(II) complex, providing the necessary driving force for reductive elimination and facilitating the formation of Ni(0) species. For example, the Guan group reported a computational study of Ni(0)/Lewis acid catalysed polyfluoroarylcyanation of alkynes.[63]

In this case, the BPh_3 serves as a Lewis acid, significantly contributing to the acceleration of the reaction. The calculated free energy profiles are shown in Fig. 4, which starts from Ni(II) species **12**. The alkyne substrate coordinates with the Ni(II) center of **12** to give intermediate **13**, which then undergoes alkyne insertion *via* transition state **14-ts** to generate Ni(II)-alkenyl intermediate **15** with an energy barrier of 19.6 kcal mol^{-1}. After that, the tri-coordinated intermediate **15** transforms to tetra-coordinated intermediate **16**, which then undergoes Lewis acid assisted reductive elimination *via* a three-membered-ring transition state **17-ts** with an energy barrier of only 11.4 kcal mol^{-1}. Geometry analysis shows that the length of the N–B bond is 1.58 Å, which indicates an obvious interaction

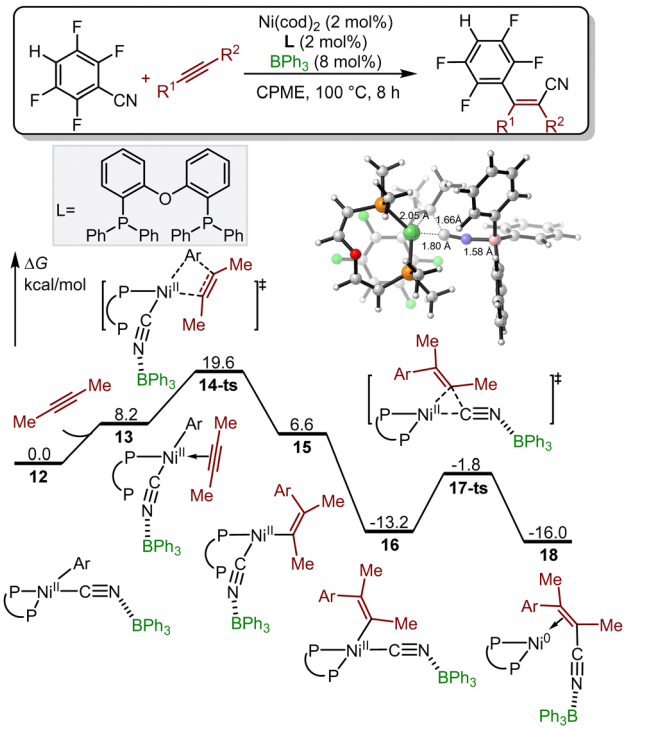

Fig. 4 Free energy profiles of Ni/Lewis acid-catalysed polyfluoroaryl cyanation of alkynes. The energies were calculated at the M06/6-311++G(2d,2p) (SDD for Ni)/CMCP(diethyl ether)//M06/6-31++G(d,p) (LANL2DZ for Ni) level of theory.

between the cyano group and electron-deficient BPh_3. The presence of a Lewis acid enhances the charge transfer from the substrate to the Ni atom center, thereby facilitating the reductive elimination from Ni(II) species.

3.2. Z-type ligand-assisted reductive elimination from Ni(II) species

Z-Type ligands are typically defined as Lewis acidic metals or metalloids that serve as σ-acceptor ligands, which can exhibit dative bonding with late transition metals. The Z-type coordination activates the transition metal electrophilically by withdrawing electron density from the filled d-orbital. This is distinct from standard organic ligands such as phosphines and amines, which usually coordinate to transition metals mainly through σ-donation and in some cases through secondary π-back donation. In Ni catalysed cross-coupling, Z-type coordination can reduce the overall electron density of the Ni atom, enhancing the driving force of reductive elimination from Ni(II) species.

For example, our group performed a theoretical study on the mechanism of $C(sp^3)$–$C(sp^3)$ reductive elimination from Ni(II) species with the assistance of a Z-type metalloligand (Scheme 5).[62]

In this reaction, computational evidence supports a mechanism in which Zn coordinates onto the Ni center as a Z-type ligand accelerating reductive elimination. This Z-type ligand assisted pathway is found to be lower in energy compared with

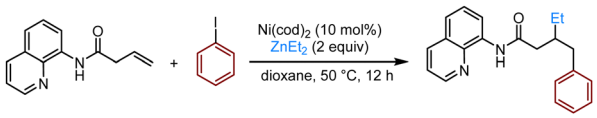

Scheme 5 Ni-catalysed 1,2-arylalkylation of olefins with organozinc reagents.

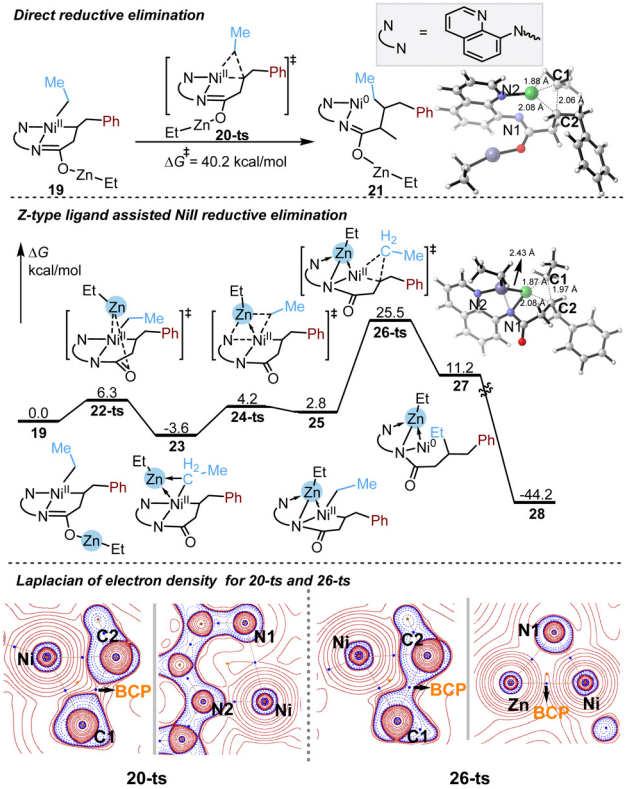

Fig. 5 Free energy profiles of the key step of Z-type ligand-assisted reductive elimination from Ni(II) species. The energies were calculated at the M06/6-311+G(d) (LANL08+ for Ni and Zn, SDD for I)/SMD(dioxane)//B3LYP/6-31G(d)/SDD(for Ni, Zn, and I) level of theory.

direct reductive elimination from a σ-coordinated Ni(II) species. The key steps for reductive elimination are shown in Fig. 5. Both the direct and Z-type ligand-assisted reductive elimination pathways were calculated in this work. The direct reductive elimination occurs *via* a three-membered-ring transition state **20-ts** with an energy barrier of 40.2 kcal mol^{-1}, which indicates that the direct reductive elimination is difficult to achieve under the reported reaction conditions (50 °C, 12 h). Alternatively, the Z-type ligand assisted reductive elimination is also considered. An intramolecular Zn shift could occur *via* transition state **22-ts**, resulting in the formation of a Ni–Zn Z-type dative bond in intermediate **23**. The Z-type datively bound organozinc ligand in intermediate **23** can insert into the Ni–N bond *via* isomerization transition state **24-ts** to give an N–Ni–Zn three-membered-ring intermediate. Z-type ligand assisted $C(sp^3)$–$C(sp^3)$ reductive elimination then occurs *via* transition state **26-ts** to form Zn–Ni(0) intermediate **27**. Geometry analysis

shows that the bond length of the Zn–Ni bond is 2.43 Å. The total activation free energy for this step is 29.1 kcal mol^{-1}, which is 11.1 kcal mol^{-1} lower than that of the direct reductive elimination. The Laplacians of the electron density in the planes defined by C1, C2, and Ni of transition states **20-ts** and **26-ts** are shown in Fig. 5. The electron density around C1 is significantly polarized toward the C2 center in transition state **26-ts** compared with that in transition state **20-ts**. This difference indicates that there is a stronger mutual attraction between C1 and C2 in **26-ts** than in **20-ts**. Apart from this, in **26-ts**, the BCP was detected in the Ni–Zn bond with a $\nabla^2\rho$ value of 0.54, which was identified in the Ni–Zn bond. Theoretical calculations indicate a significant Z-type Ni–Zn interaction that reduces the electron density around the Ni center and accelerates reductive elimination.

3.3. π-acid ligand-assisted reductive elimination of Ni(II) species

π-acidic ligands, such as CO, alkenes, and alkynes, feature empty or partially filled π* (antibonding) orbitals capable of accepting electrons from the d orbitals of Ni(II), which could also be named as a back-donation bond. This electron withdrawing property can reduce the electron density at the Ni(II) center, enhancing its electrophilicity and thereby increasing the driving force for reductive elimination.

For example, a comprehensive experimental and theoretical investigation conducted by Chatani and our group has revealed that the coordination of π-acidic ligands diphenylacetylene to the Ni(II) center has been found to significantly promote the reductive elimination.[83] The key step for reductive elimination is shown in Fig. 6. When Ni(II) intermediate **29** is formed, the migratory insertion into the Ni–C(aryl) bond with diphenylacetylene occurs to give the Ni(II)-alkenyl intermediate **31**, which then isomerizes into the seven-membered-ring Ni(II)-vinyl intermediate **32**. Subsequently, π-acidic ligand-assisted reductive elimination takes place *via* the transition state **33-ts** with an energy barrier of only 10.6 kcal mol^{-1} to give the η^3-coordinated Ni(0) species **34**. Notably, during the catalytic cycle, alkyne serves not only as a substrate but also as a π-acidic ligand coordinating with the Ni(II) center. This coordination effectively reduces the electron density of the Ni(II) center, thereby significantly facilitating the reductive elimination of Ni(II) species.

Additionally, in Ni-catalysed cross-coupling reactions, alkenes can also serve as π-acidic ligands, promoting the reductive elimination of Ni(II) species. As an example, Li and our group have reported mechanistic studies on Ni-catalysed enantioselective [3+2] annulation.[68] In this work, we found that the enone substrate can also serve as a π-acidic ligand, facilitating the reductive elimination of Ni(II) species. The DFT calculated free energy profiles for the key step of this reaction are shown in Fig. 7. The reaction starts from Ni(0) species **35**, which undergoes oxidative addition of cyclopropenone *via* transition state **36-ts** to give Ni(II) intermediate **37**. Subsequently, 4,1-insertion of enone into the Ni–C bond occurs *via* transition state **38-ts** to form the Ni(II)-allyl intermediate **39**. The π-acidic ligand-assisted reductive elimination takes place *via* transition state **40-ts** to afford the Ni(0) intermediate **41**. Geometry analysis of transition state **40-ts** reveals a strong coordination interaction between the enone and the Ni(II) during the reductive elimination process. Due to the stabilization of the resulting Ni(0) species by the coordinated π-acidic alkenyl ligands, the energy barrier

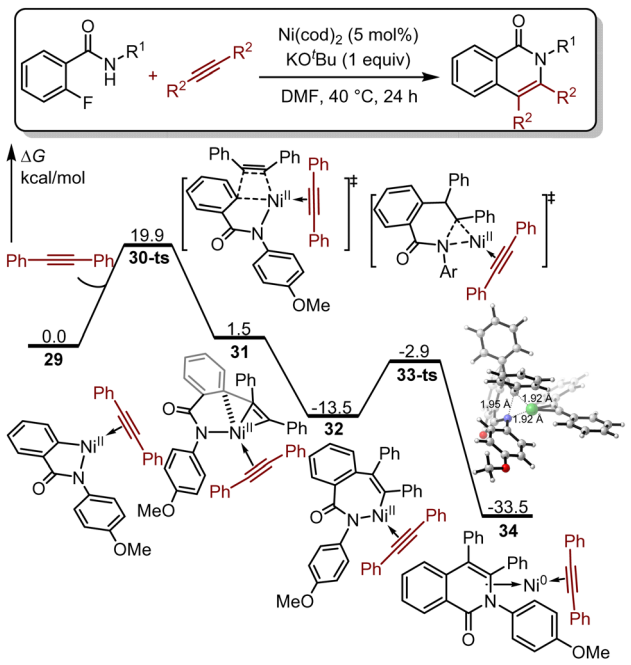

Fig. 6 Free energy profiles of Ni-catalysed C–F bond activation of aromatic amides with alkynes. The energies were calculated at the M06/6-311+G(d) (LANL08 for Ni)/SMD(DMF)//B3LYP/6-31G(d) (LANL08 for Ni) level of theory.

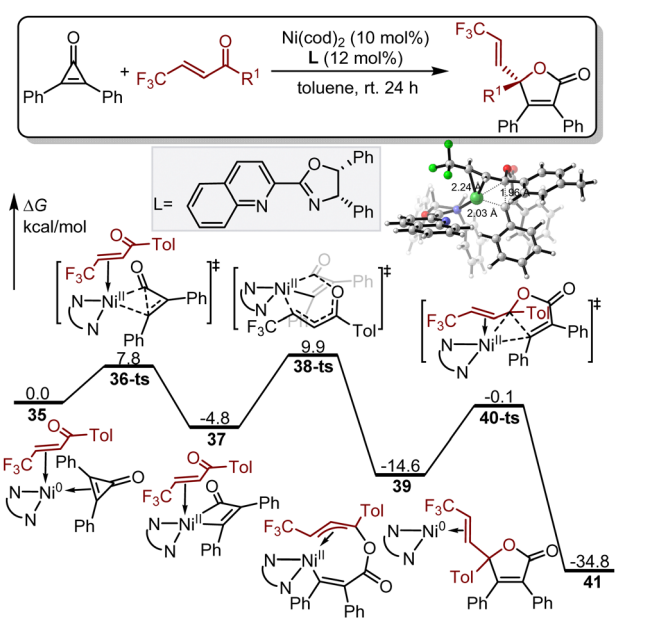

Fig. 7 Free energy profiles of Ni-catalysed enantioselective [3+2] annulation for γ-butenolide synthesis *via* C–C activation of diarylcyclopropenones. The energies were calculated at the M06/6-311+G(d,p) (LANL08 for Ni)/SMD(toluene)//B3LYP/6-31G(d) (LANL08 for Ni) level of theory.

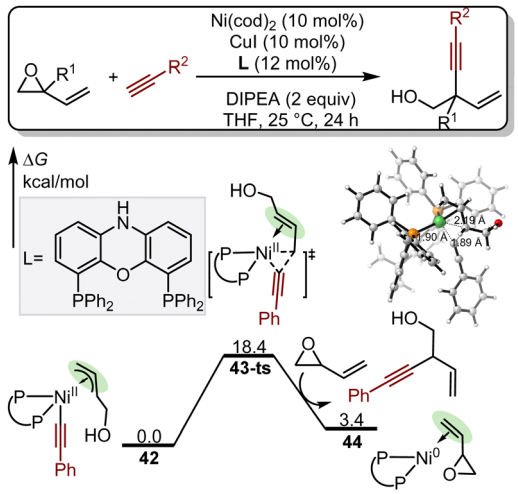

Fig. 8 Free energy profile of Ni-catalysed allylic alkylations of alkynes. The energies were calculated at the M11-L/6-311+G(d) (SDD for Ni)/SMD(toluene)//B3LYP/6-31G(d) (SDD for Ni) level of theory.

for π-acidic ligand-assisted reductive elimination is only 14.5 kcal mol^{-1}.

In another example, we revealed the mechanism of Ni-catalysed allylic alkylations of alkynes (Fig. 8).[67] In our mechanistic investigation, we hypothesize that the vinyl epoxide could serve as a potential π-allyl ligand to accelerate the reductive elimination from Ni(II) species. DFT calculation verified our speculation that the π-acidic ligand-assisted reductive elimination proceeds *via* transition state **43-ts** with an energy barrier of 18.4 kcal mol^{-1} to give the internal alkylation product **44**. The calculated result indicates that the π-acidic ligand-assisted reductive elimination is conducive to the formation of C(alkynyl)–C(allyl) bonds in the current reaction.

4. Oxidation induced reductive elimination from Ni(II) species

Another effective approach to enhance the reductive elimination ability of Ni(II) species is to modify the oxidation state of the Ni atom. Oxidation induced reductive elimination of Ni(II) species represents a mechanism wherein the reductive elimination process is facilitated through an oxidative pathway. In this context, Ni(II) species are oxidized to higher oxidation states, such as Ni(III) or Ni(IV), in the presence of an oxidizing agent.[84,85] This pathway can reduce the electron density at the Ni center, making it more electrophilic and thereby enhancing its ability to accept electrons. As a result, the driving force for reductive elimination is significantly increased.

The general mechanism of oxidation-induced reductive elimination from Ni(II) species is shown in Scheme 6. Based on the mode of oxidation, two types of oxidation induced reductive elimination pathways are proposed. In single-electron oxidation induced reductive elimination mode E (green lines), single-electron oxidation of Ni(II) species occurs with a radical species to give the Ni(III) intermediate, which then undergoes

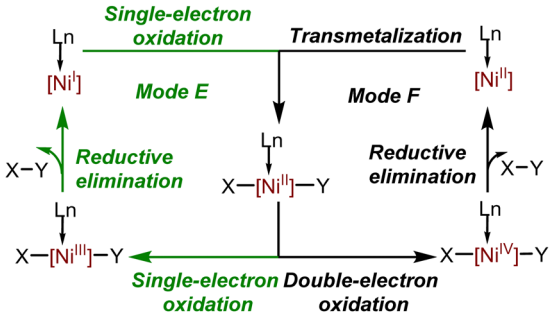

Scheme 6 General mechanism of oxidation-induced reductive elimination from Ni(II) species.

reductive elimination to afford the Ni(I) intermediate with concomitant formation of the coupling product. After that, another single-electron oxidation of the Ni(I) intermediate occurs to regenerate the Ni(II) species. Alternatively, in double-electron oxidation-induced reductive elimination mode F (black lines), double-electron addition of Ni(II) species occurs with an electrophile to generate the Ni(IV) intermediate, which then undergoes reductive elimination to afford another Ni(II) intermediate with concomitant formation of the coupling product. After that, the active Ni(II) species can be regenerated through transmetalization.

4.1. Single-electron oxidation induced reductive elimination

A combined experimental and theoretical study by Xiao and our group found that the single-electron oxidation-induced reductive elimination pathway is more favorable than direct reductive elimination from Ni(II) species.

The DFT calculated free energy profiles for the key steps of this reaction are shown in Fig. 9.[86] In single-electron oxidation induced reductive elimination, oxidative addition of Ni(0) species occurs to give the Ni(II)-aryl intermediate **47**, which can be oxidized by the excited *[Ir(III)]$^+$ photocatalyst through single-electron-transfer (SET) to afford Ni(III) intermediate **48**. After that, α-aminoacetonitrile coordinates to intermediate **48** to form intermediate **49**, which then undergoes C–C bond cleavage *via* transition state **50-ts** to generate the Ni(III)-isocyano intermediate **51** with the release of the iminium cation. Subsequent isomerization proceeds *via* transition state **52-ts** to form the Ni(III)-cyano species **53**. The reductive elimination takes place *via* a three-membered-ring transition state **54-ts** with an energy barrier of only 2.7 kcal mol^{-1}. On the other hand, we also calculated the direct reductive elimination from Ni(II) species. Interestingly, the activation free energy of transition state **57-ts** for this step is 29.4 kcal mol^{-1}, which is 26.7 kcal mol^{-1} higher than that of the reductive elimination *via* transition state **54-ts**. The calculated result illustrates the superiority of the mechanism for oxidation-induced reductive elimination from Ni(II) species.

In Ni-catalysed cross-coupling reaction, alkyl halides are potential sources of alkyl radicals and may undergo a single-electron oxidation process during the catalytic cycle. For example, a collaboration between Koh and our group reported Ni-catalysed

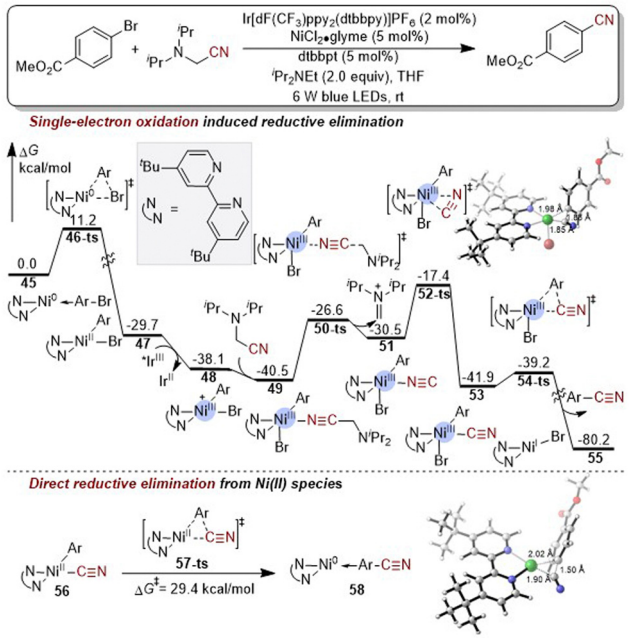

Fig. 9 Free energy profiles of cyanation of aryl halides by dual photoredox and Ni catalysis. The energies were calculated at the M06/6-311+G(d,p) (SDD for Ni and Ir)/SMD(THF)//B3LYP/6-31G(d) (SDD for Ni and Ir) level of theory.

regioselective alkene dialkylation. In this reaction, the alkyl iodides can serve as an oxidizing agent.[87] By promoting the single-electron oxidation of Ni(II) to Ni(III) species, the reductive elimination of Ni(III) species is facilitated. DFT calculation revealed the mechanism of single-electron oxidation-induced reductive elimination (Fig. 10). When iodoethane is situated close to Ni(I)-alkyl complex **59**, an inner-sphere-single-electron transfer (ISET)-assisted homolytic C–I bond cleavage could occur *via* transition state **60-ts** to release an ethyl radical and

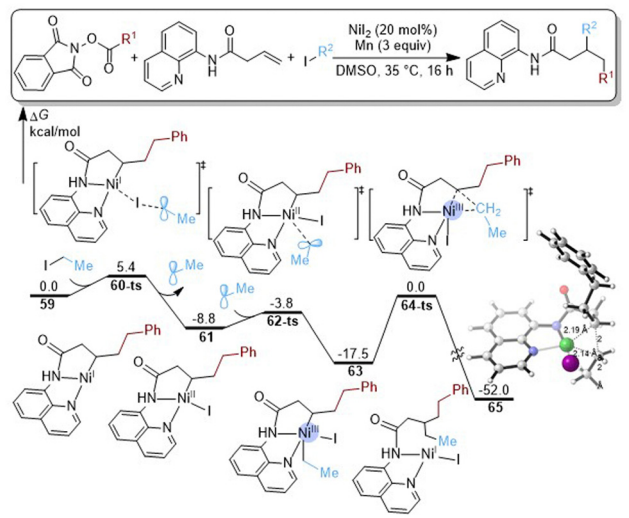

Fig. 10 Free energy profiles of the key step of Ni-catalysed regioselective alkene dialkylation. The energies were calculated at the M06L/def2-TZVPP/SMD(DMSO)//B3LYP/def2-SVP level of theory.

form an iodo-Ni(II)-alkyl intermediate **61**. The single-electron oxidation of **61** with an ethyl radical occurs *via* transition state **62-ts** to generate a Ni(III)-dialkyl intermediate **63**, which can undergo reductive elimination to achieve the alkylation. The total activation free energy for reductive elimination *via* transition state **64-ts** is 17.5 kcal mol^{-1}.

In another example, Koh and our group reported Ni catalysed multicomponent synthesis of C-acyl glycosides. A combined experimental and theoretical study revealed the reaction mechanism, further demonstrating the broad applicability of single-electron oxidation-induced reductive elimination.[51] The calculated free energy profiles are shown in Fig. 11. Ni(I)-Acyl intermediate **66** can react with D-mannofuranosyl chloride **1** *via* a halogen atom transfer (XAT) transition state **67-ts** to furnish a glycosyl radical and a Ni(II) intermediate **68**. Subsequently, single-electron oxidation of intermediate **68** with a glycosyl radical occurs *via* transition state **69-ts** to form a Ni(III) intermediate **70**. Following that, Ni(III) intermediate **70** undergoes reductive elimination *via* transition state **71-ts**, resulting in the formation of the carbonylative cross-coupling product. The total activation free energy for reductive elimination *via* transition state **71-ts** is only 14.1 kcal mol^{-1}. These results corroborate the aforementioned conclusion that the single-electron oxidation induced reductive elimination has a low energy barrier, which can be attributed to the high oxidizing ability of Ni(III) species.

4.2. Double-electron oxidation induced reductive elimination

In Ni-catalysed cross coupling reactions, the presence of strong oxidizing agents or strong electron-donating ligands can oxidize Ni(II) species to Ni(IV) species, enabling a double-electron oxidation induced reductive elimination. As an example, our group revealed the mechanism of Ni-catalysed C–H arylation

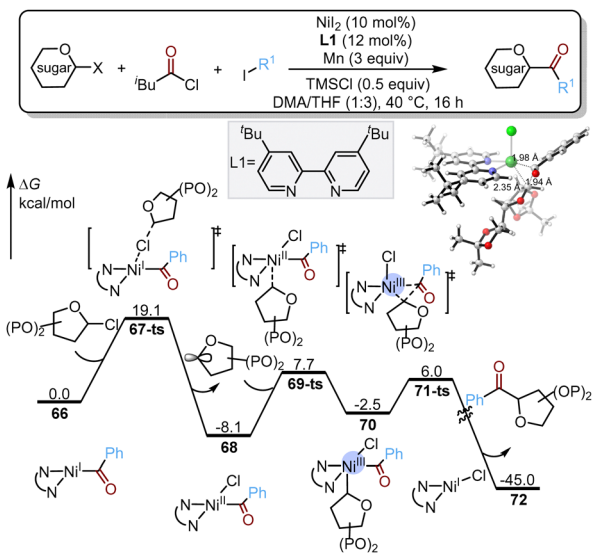

Fig. 11 Free energy profiles of the key step of Ni-catalysed synthesis of C-acyl glycosides. The energies were calculated at the B3LYP/6-311+G(d,p) (LANL08 for Ni and I)/IEF-PCM(DMA)//B3LYP/6-31G(d) (LANL2DZ for Ni and I)/IEF-PCM(DMA) level of theory.

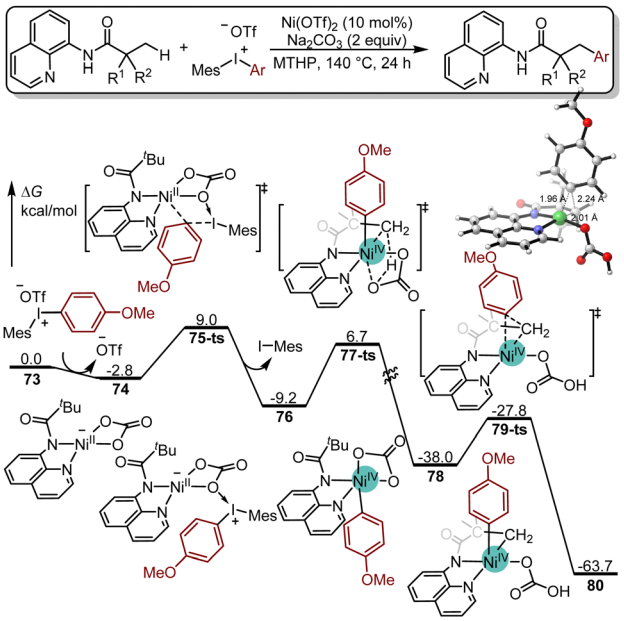

Fig. 12 Free energy profiles of the key step of Ni-catalysed C–H arylation with diaryliodonium salts or phenyliodides involved. The energies were calculated at the M11-L/6-311+G(d) (SDD for Ni and I)/SMD(dioxane)//B3LYP/6-31+G(d) (SDD for Ni and I) level.

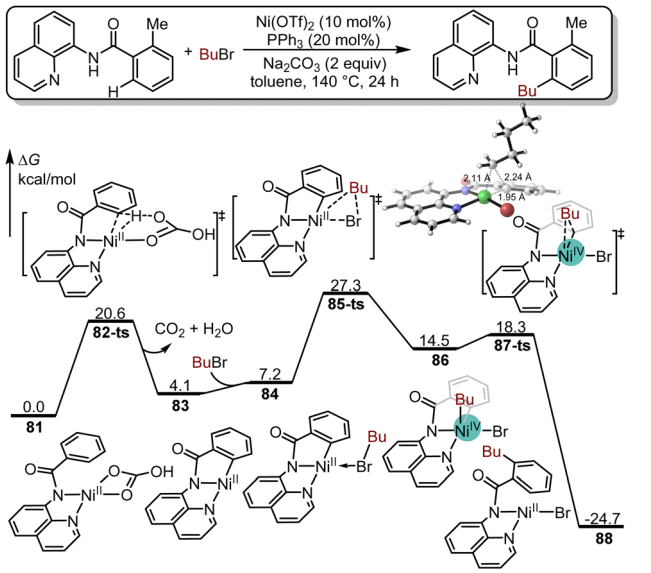

Fig. 13 Free energy profiles of the key step of Ni-catalysed alkylation of benzamides with alkyl halides. The energies were calculated at the B3LYP-D3/6-311++G(d,p) (SDD for Ni)/SMD(toluene)//B3LYP/6-31+G(d) (LANL2DZ for Ni) level.

with diaryliodonium.[88] Due to the strong oxidizing properties of diaryliodonium salt, Ni(II) species can be oxidized to Ni(IV) species, enhancing the driving force of reductive elimination. The free energy profiles of double-electron oxidation-induced reductive elimination are presented in Fig. 12. By the coordination of a diaryliodonium salt, OTf^- is replaced in Ni(II) complex **73** to form neutral Ni(II) intermediate **74**, which then undergoes oxidative addition *via* concerted six-membered-type transition state **75-ts** to generate the more stable aryl-Ni(IV) intermediate **76** with the concomitant release of MesI. Subsequently, carbonate-assisted C–H bond cleavage of intermediate **76** generates the Ni(IV) intermediate **78** *via* transition state **77-ts**. Finally, the reductive elimination of the alkyl group and aryl group on Ni occurs *via* a concerted three-membered ring-type transition state **79-ts** to yield cross-coupling product **80**. The activation free energy for reductive elimination from Ni(IV) species is only 10.2 kcal mol^{-1}, which further demonstrates that the double-electron oxidation-induced reductive elimination pathway is highly favourable.

Due to the electron-rich framework of pyridine ligands, their cyclic structure offers strong coordination ability, aiding in the stabilization of Ni(IV) species. In the presence of these ligands, the double-electron oxidation induced reductive elimination pathway must be considered. For example, we performed a theoretical study on the mechanism of Ni-catalysed alkylation of benzamides with alkyl halides.[89] The 8-aminoquinoline (AQ) directing group serves as a strong ligand during the catalytic cycle, facilitating the double-electron oxidation-induced reductive elimination. As shown in Fig. 13, when amide anion coordination complex **81** is formed, subsequent C–H bond activation *via* the transition state **82-ts** affords an electronically unsaturated tri-coordinate-Ni intermediate **83**. Next, the coordination of one BuBr molecule forms the planar complex **84**, which then undergoes oxidative addition *via* the transition state **85-ts** to give the high-valent Ni(IV) intermediate **86**. The high-valent and highly active Ni(IV) intermediate **86** leads to a lowering of the energy barrier by 3.8 kcal mol^{-1} for reductive elimination *via* transition state **87-ts**. Notably, the oxidative addition of Ni(II) to form high valent Ni(IV) species was often considered to be the rate-determining step in this type of Ni-catalysed coupling reaction.

5. Conclusions and outlooks

During the past two decades, Ni-catalysed coupling reactions have been extensively reported, and their corresponding mechanistic studies have garnered considerable attention. Reductive elimination, being the final step in the formation of covalent bonds within these reactions, represents a pivotal phase in mechanistic studies. Due to the weak oxidizing ability of Ni(II) species, reductive elimination from Ni(II) species is typically challenging. Exploring the reductive elimination mechanisms of Ni(II) species and pinpointing the critical factors that enhance this process can unveil new opportunities for the design and development of Ni-catalysed coupling reactions.

In this work, we provide a comprehensive summary of recent advances in the computational study of reductive elimination from Ni(II) species. Three typical reaction models for reductive elimination from Ni(II) species were investigated and discussed, including direct reductive elimination, electron density-controlled reductive elimination, and oxidation-induced reductive elimination. The computational results showed that the direct reductive elimination mode is predominantly observed

in cross-coupling with C(sp^2) electrophiles. Owing to the insufficient driving force for reductive elimination in this mode, the formation of new covalent bonds usually encounters a high energy barrier. Notably, the electron density-controlled reductive elimination model can enhance the driving force for reductive elimination of Ni(II) species by finely regulating the electronic environment of the Ni center. This model can be further classified into Lewis acid, Z-type ligand, and π-acid ligand-assisted reductive elimination. Theoretical calculations have demonstrated that reductive elimination of Ni(II) species is significantly facilitated under these modes. Moreover, the oxidation-induced reductive elimination model can promote the transformation of Ni(II) species to more reactive Ni(III) and Ni(IV) species, thereby reducing the energy barrier for reductive elimination. This transformation is facilitated by single-electron oxidation or oxidative addition in the presence of radical species or oxidizing agents, respectively. Depending on the type of oxidation, this model can be further categorized into single-electron oxidation-induced and double-electron oxidation-induced reductive elimination mechanisms. Theoretical calculations have elucidated the viability of these mechanisms in detail. These three reductive elimination models have elucidated the complexity of the reductive elimination from Ni(II) species and identified effective strategies for enhancing the driving force of this step. Future research on Ni-catalysed coupling reactions should prioritize the integration of computational and experimental studies to explore the feasibility of additional Ni-catalysed reductive elimination pathways. This integrated approach will facilitate the optimization of catalytic conditions, enhance reaction efficiency and selectivity, and further promote the practical applications of Ni-catalysed coupling reactions.

Author contributions

Conceptualization: B. Q., F.-Y. L., D. F., S.-J. L., Y. L.; Writing – original draft: B. Q., F.-Y. L., T. Z.; Writing – review & editing: T. Z., Y. L.; Visualization: B. Q., F.-Y. L.; Supervision: T. Z., Y. L.; Project administration: Y. L.; Funding acquisition: Y. L. All authors read and approved the final manuscript.

Data availability

No primary research results, software or code have been included and no new data were generated or analysed as part of this feature article.

Conflicts of interest

There are no conflicts to declare.

Acknowledgements

This work was supported by the National Natural Science Foundation of China (Grants 22303099 and 21903071), the Joint Fund of Key Technologies Research & Development Program of Henan Province (Grant 222301-420006), the Fundamental Research Fund of Henan Academy of Sciences (240626008) and the Ministry of Science and Technology of the People's Republic of China.

Notes and references

1 J. Choi and G. C. Fu, *Science*, 2017, **356**, eaaf7230.
2 L. Peng, Z. Hu, Z. Tang, Y. Jiao and X. Xu, *Chin. Chem. Lett.*, 2019, **30**, 1481–1487.
3 K. Ouyang, W. Hao, W.-X. Zhang and Z. Xi, *Chem. Rev.*, 2015, **115**, 12045–12090.
4 Z. Zuo, D. T. Ahneman, L. Chu, J. A. Terrett, A. G. Doyle and D. W. C. MacMillan, *Science*, 2014, **345**, 437–440.
5 K. Wu, D. Lu, J. Lin, T.-B. Wen, W. Hao, K. Tan and H.-J. Zhang, *Chin. Chem. Lett.*, 2024, **35**, 108906.
6 Y. Xia, D. Qiu and J. Wang, *Chem. Rev.*, 2017, **117**, 13810–13889.
7 Y. Xia and J. Wang, *J. Am. Chem. Soc.*, 2020, **142**, 10592–10605.
8 Y.-Z. Yang, G.-F. Lv, M. Hu, Y. Li and J.-H. Li, *Chin. Chem. Lett.*, 2023, **34**, 108590.
9 T. Liu, R. Duan, Y. Wang, S. Li, L. Qu, J. Song, Q. Liu and Y. Lan, *Chin. Chem. Lett.*, 2022, **33**, 4281–4286.
10 Z. Zeng, R. Bai, Y. Lan, X. He, K. Zhong, D. Heng and H. Ni, *Chin. Chem. Lett.*, 2022, **33**, 2031–2035.
11 P. Chen, L. Liang, Y. Zhu, Z. Xing, Z. Jia and T.-P. Loh, *Chin. Chem. Lett.*, 2024, **35**, 109229.
12 X. Qi and Y. Lan, *Chin. J. Org. Chem.*, 2022, **42**, 1258–1259.
13 K. Zhong, S. Liu, X. He, H. Ni, W. Lai, W. Gong, C. Shan, Z. Zhao, Y. Lan and R. Bai, *Chin. Chem. Lett.*, 2023, **34**, 108339.
14 C. Liu, C. Liu, X.-M. Li, Z.-M. Gao and Z.-L. Jin, *Chin. Chem. Lett.*, 2016, **27**, 631–634.
15 L. Jin, J. Han, D. Fang, M. Wang and J. Liao, *Chin. Chem. Lett.*, 2024, **35**, 109212.
16 R. Chinchilla and C. Nájera, *Chem. Rev.*, 2014, **114**, 1783–1826.
17 X. Ma, J. Su and Q. Song, *Acc. Chem. Res.*, 2023, **56**, 592–607.
18 A. Biffis, P. Centomo, A. Del Zotto and M. Zeccal, *Chem. Rev.*, 2018, **118**, 2249–2295.
19 I. P. Beletskaya, F. Alonso and V. Tyurin, *Coord. Chem. Rev.*, 2019, **385**, 137–173.
20 D. Haas, J. M. Hammann, R. Greiner and P. Knochel, *ACS Catal.*, 2016, **6**, 1540–1552.
21 N. D. Schley and G. C. Fu, *J. Am. Chem. Soc.*, 2014, **136**, 16588–16593.
22 D. Wang, A. B. Weinstein, P. B. White and S. S. Stahl, *Chem. Rev.*, 2018, **118**, 2636–2679.
23 R.-X. Liang and Y.-X. Jia, *Acc. Chem. Res.*, 2022, **55**, 734–745.
24 J. Peng, X. He, L.-L. Liao, R. Bai and Y. Lan, *Chin. J. Org. Chem.*, 2023, **43**, 3608–3613.
25 V. M. Chernyshev and V. P. Ananikov, *ACS Catal.*, 2022, **12**, 1180–1200.
26 N. A. Weires, E. L. Baker and N. K. Garg, *Nat. Chem.*, 2016, **8**, 75–79.
27 Y. Lan, *Computational Methods in Organometallic Catalysis*, Wiley-VCH Press, Germany, 2021.
28 Y. Xiao, W. Huang and Q. Shen, *Chin. Chem. Lett.*, 2022, **33**, 4277–4280.
29 C. S. Day, A. Renteria-Gomez, S. J. Ton, A. R. Gogoi, O. Gutierrez and R. Martin, *Nat. Catal.*, 2023, **6**, 244–253.
30 Z. Zhao, J. Liu, C.-H. Tung and W. Wang, *Chin. Chem. Lett.*, 2023, **34**, 108293.
31 Q. Pan, Y. Y. Ping and W. Q. Kong, *Acc. Chem. Res.*, 2023, **56**, 515–535.
32 S. Z. Tasker, E. A. Standley and T. F. Jamison, *Nature*, 2014, **509**, 299–309.
33 J. Derosa, O. Apolinar, T. Kang, V. T. Tran and K. M. Engle, *Chem. Sci.*, 2020, **11**, 4287–4296.
34 D. Balcells and A. Nova, *ACS Catal.*, 2018, **8**, 3499–3515.
35 V. P. Ananikov, *ACS Catal.*, 2015, **5**, 1964–1971.
36 C.-Y. Lin and P. P. Power, *Chem. Soc. Rev.*, 2017, **46**, 5347–5399.
37 B. Zheng, F. Tang, J. Luo, J. W. Schultz, N. P. Rath and L. M. Mirica, *J. Am. Chem. Soc.*, 2014, **136**, 6499–6504.
38 N. M. Camasso and M. S. Sanford, *Science*, 2015, **347**, 1218–1220.

39 J. B. Diccianni, J. Katigbak, C. Hu and T. Diao, *J. Am. Chem. Soc.*, 2019, **141**, 1788–1796.
40 S. K. Kariofillis, S. T. Jiang, A. M. Zuranski, S. S. Gandhi, J. I. M. Alvarado and A. G. Doyle, *J. Am. Chem. Soc.*, 2022, **144**, 1045–1055.
41 J. B. Mann, T. L. Meek, E. T. Knight, J. F. Capitani and L. C. Allen, *J. Am. Chem. Soc.*, 2000, **122**, 5132–5137.
42 M. Tobisu and N. Chatani, *Acc. Chem. Res.*, 2015, **48**, 1717–1726.
43 J. Diccianni, Q. Lin and T. Diao, *Acc. Chem. Res.*, 2020, **53**, 906–919.
44 J. B. Diccianni and T. N. Diao, *Trends Chem.*, 2019, **1**, 830–844.
45 J. E. Dander and N. K. Garg, *ACS Catal.*, 2017, **7**, 1413–1423.
46 L. M. Wickham and R. Giri, *Acc. Chem. Res.*, 2021, **54**, 3415–3437.
47 J. F. Hartwig, *Inorg. Chem.*, 2007, **46**, 1936–1947.
48 S. Jin, J. Kim, D. Kim, J.-W. Park and S. Chang, *ACS Catal.*, 2021, **11**, 6590–6595.
49 C. Zhu, H. F. Yue, J. Q. Jia and M. Rueping, *Angew. Chem., Int. Ed.*, 2021, **60**, 17810–17831.
50 S. Chen, X. He, C. Jin, W. Zhang, Y. Yang, S. Liu, Y. Lan, K. N. Houk and X. Shen, *Angew. Chem., Int. Ed.*, 2022, **61**, e202213431.
51 Y. Jiang, K. Yang, Y. Wei, Q. Wang, S. J. Li, Y. Lan and M. J. Koh, *Angew. Chem., Int. Ed.*, 2022, **61**, e202211043.
52 Y.-J. Dong, Z.-W. Zhao, Y. Geng, Z.-M. Su, B. Zhu and W. Guan, *Inorg. Chem.*, 2023, **62**, 1156–1164.
53 H. M. Omer and P. Liu, *ACS Omega*, 2019, **4**, 5209–5220.
54 W. Shu, A. García-Domínguez, M. T. Quirós, R. Mondal, D. J. Cárdenas and C. Nevado, *J. Am. Chem. Soc.*, 2019, **141**, 13812–13821.
55 B. Qiao, R. Bai, T. Zhang, S.-J. Li and Y. Lan, *Mol. Catal.*, 2022, **526**, 112378.
56 Z.-J. Zhang, M. M. Simon, S. Yu, S.-W. Li, X. Chen, S. Cattani, X. Hong and L. Ackermann, *J. Am. Chem. Soc.*, 2024, **146**, 9172–9180.
57 M. C. Schwarzer, R. Konno, T. Hojo, A. Ohtsuki, K. Nakamura, A. Yasutome, H. Takahashi, T. Shimasaki, M. Tobisu, N. Chatani and S. Mori, *J. Am. Chem. Soc.*, 2017, **139**, 10347–10358.
58 V. T. Tran, Z. Q. Li, T. J. Gallagher, J. Derosa, P. Liu and K. M. Engle, *Angew. Chem., Int. Ed.*, 2020, **59**, 7029–7034.
59 R. K. Dhungana, R. R. Sapkota, L. M. Wickham, D. Niroula and R. Giri, *J. Am. Chem. Soc.*, 2020, **142**, 20930–20936.
60 Q. Wang, K.-B. Zhong, H. Xu, S.-N. Li, W.-K. Zhu, F. Ye, Z. Xu, Y. Lan and L.-W. Xu, *ACS Catal.*, 2022, **12**, 4571–4580.
61 Z. Q. Li, Y. Fu, R. Deng, V. T. Tran, Y. Gao, P. Liu and K. M. Engle, *Angew. Chem., Int. Ed.*, 2020, **59**, 23306–23312.
62 T. Zhang, K. Zhong, Z.-K. Lin, L. Niu, Z.-Q. Li, R. Bai, K. M. Engle and Y. Lan, *J. Am. Chem. Soc.*, 2023, **145**, 2207–2218.
63 H. Ren, G.-F. Du, B. Zhu, G.-C. Yang, L.-S. Yao, W. Guan and Z.-M. Su, *Organometallics*, 2018, **37**, 2594–2601.
64 Y. Li, H. Liang, Y. Liu, J. Lin and Z. Ke, *ACS Catal.*, 2023, **13**, 13008–13020.
65 L. Yang, K. Fan, L. Zhang and G. Zeng, *Mol. Syst. Des. Eng.*, 2022, **7**, 780–787.
66 Q. Lu, H. Yu and Y. Fu, *J. Am. Chem. Soc.*, 2014, **136**, 8252–8260.
67 Y. Huang, C. Ma, S. Liu, L.-C. Yang, Y. Lan and Y. Zhao, *Chem*, 2021, **7**, 812–826.
68 D. Bai, S. Liu, J. Chen, Y. Yu, M. Wang, J. Chang, Y. Lan and X. Li, *Org. Chem. Front.*, 2021, **8**, 3023–3031.
69 J.-J. Chen, J.-H. Fang, X.-Y. Du, J.-Y. Zhang, J.-Q. Bian, F.-L. Wang, C. Luan, W.-L. Liu, J.-R. Liu, X.-Y. Dong, Z.-L. Li, Q.-S. Gu, Z. Dong and X.-Y. Liu, *Nature*, 2023, **618**, 294–300.
70 J.-J. Chen, J.-Y. Zhang, J.-H. Fang, X.-Y. Du, H.-D. Xia, B. Cheng, N. Li, Z.-L. Yu, J.-Q. Bian, F.-L. Wang, J.-J. Zheng, W.-L. Liu, Q.-S. Gu, Z.-L. Li and X.-Y. Liu, *J. Am. Chem. Soc.*, 2023, **145**, 14686–14696.
71 A. J. Hickman and M. S. Sanford, *Nature*, 2012, **484**, 177–185.
72 L. Anghileri, H. Baunis, A. R. Bena, C. Giannoudis, J. H. Burke, S. Reischauer, C. Merschjann, R. F. Wallik, G. Simionato, S. Kovalenko, L. Dell'Amico, R. M. van der Veen and B. Pieber, *chemRxiv*, 2024, DOI: **10.26434/chemrxiv-2024-896n0**.
73 B. Maity, T. R. Scott, G. D. Stroscio, L. Gagliardi and L. Cavallo, *ACS Catal.*, 2022, **12**, 13215–13224.
74 R. Li, C. X. Yang, B. H. Niu, L. J. Li, J. M. Ma, Z. L. Li, H. Jiang and W. M. Cheng, *Org. Chem. Front.*, 2022, **9**, 3847–3853.
75 P. Sahni, R. Gupta, S. Sharma and A. K. Pal, *Coord. Chem. Rev.*, 2023, **474**, 214849.
76 J. R. Bour, D. M. Ferguson, E. J. McClain, J. W. Kampf and M. S. Sanford, *J. Am. Chem. Soc.*, 2019, **141**, 8914–8920.
77 S. K. Kariofillis and A. G. Doyle, *Acc. Chem. Res.*, 2021, **54**, 988–1000.
78 N. Hazari, P. R. Melvin and M. M. Beromi, *Nat. Rev. Chem.*, 2017, **1**, 0025.
79 J. A. Milligan, J. P. Phelan, S. O. Badir and G. A. Molander, *Angew. Chem., Int. Ed.*, 2019, **58**, 6152–6163.
80 Y. Li, Y. Luo, L. Peng, Y. Li, B. Zhao, W. Wang, H. Pang, Y. Deng, R. Bai, Y. Lan and G. Yin, *Nat. Commun.*, 2020, **11**, 417.
81 H. Xu, K. Muto, J. Yamaguchi, C. Zhao, K. Itami and D. G. Musaev, *J. Am. Chem. Soc.*, 2014, **136**, 14834–14844.
82 J. Derosa, R. Kleinmans, V. T. Tran, M. K. Karunananda, S. R. Wisniewski, M. D. Eastgate and K. M. Engle, *J. Am. Chem. Soc.*, 2018, **140**, 17878–17883.
83 I. Nohira, S. Liu, R. Bai, Y. Lan and N. Chatani, *J. Am. Chem. Soc.*, 2020, **142**, 17306–17311.
84 S. Zhu, H. Li, Y. Li, Z. Huang and L. Chu, *Org. Chem. Front.*, 2023, **10**, 548–569.
85 B. Ling, S. Yao, S. Ouyang, H. Bai, X. Zhai, C. Zhu, W. Li and J. Xie, *Angew. Chem., Int. Ed.*, 2024, e202405866.
86 Y. Jia, Y.-Y. Liu, L.-Q. Lu, S.-H. Liu, H.-B. Zhou, Y. Lan and W.-J. Xiao, *CCS Chem.*, 2022, **4**, 1577–1586.
87 T. Yang, Y. Jiang, Y. Luo, J. J. H. Lim, Y. Lan and M. J. Koh, *J. Am. Chem. Soc.*, 2020, **142**, 21410–21419.
88 T. Zhang, S. Liu, L. Zhu, F. Liu, K. Zhong, Y. Zhang, R. Bai and Y. Lan, *Commun. Chem.*, 2019, **2**, 31.
89 Y. Li, L. Zou, R. Bai and Y. Lan, *Org. Chem. Front.*, 2018, **5**, 615–622.